ELSEVIER

S0032-3861(96)00598-8

Polymer Vol. 38 No. 5, pp. 1011–1016, 1997

0032-3861/97/$17.00+0.00

Study of the polymer morphology in a poly(ester-urethane) elastomer by solid state ^{1}H n.m.r. spectroscopy

N. J. Clayden*
School of Chemical Sciences, University of East Anglia, Norwich NR4 7TJ, UK

and C. L. Nijs and G. J. Eeckhaut
ICI Polyurethanes, Everslaan 45, B-3078 Kortenberg, Belgium
(Received 16 January 1996; revised 18 April 1996)

The variation in the mobile fraction seen in the ^{1}H n.m.r. free induction decay has been analysed using the Thomson–Gibbs equation to give the hard block lamellae thickness distribution in a poly(ester-urethane) elastomer. Attempts to use ^{1}H spin diffusion to fix the absolute distance scale were unsuccessful since the results indicated a heterogeneity with not all of the soft segments contributing to a simple two phase hard/soft domain morphology. Selective ^{13}C n.m.r. experiments confirm the partitioning of the ^{1}H n.m.r signal at room temperature into rigid and mobile components from the hard and soft segments respectively. Chain extender contributes to both the rigid and mobile ^{1}H n.m.r. signal. © 1997 Elsevier Science Ltd. All rights reserved.

(Keywords: ^{1}H n.m.r.; Thomson–Gibbs; polyurethane)

INTRODUCTION

Polyurethane elastomers are characterized by a segmented structure formed by alternating flexible polyester or polyether segments and stiff segments formed in the reaction between methylenediphenyleneisocyanate (MDI) and chain extender molecules[1]. Incompatibility of these so called hard and soft segments leads to a polymer with a phase separated mesostructure composed of glassy and rubbery domains. The hard microdomains which are thought to act as rigid reinforcing particles and physical crosslink sites provide the mechanical strength. Previous studies of the domain structure by n.m.r. have concentrated on ^{1}H spin diffusion which give a mean size for the hard and soft domains[2,3]. Recently, however, a novel interpretation of the temperature dependence of the wideline ^{2}H n.m.r. spectra of a polyurethane specifically deuterated in the hard segment in terms of the Thomson–Gibbs equation has allowed domain size distributions to be determined for the first time by n.m.r.[4]. In this description, at any particular temperature the deuterated hard segments embedded in the solid hard blocks would give rise to a rigid lattice type ^{2}H n.m.r. lineshape while the hard segments liberated by the softening process of the hard blocks would give the narrow lineshape. This model is consistent with Koberstein's view that dissolution of hard domains into the soft phase can be considered as a melting process[5]. The variable melting point of the hard block lamellae is understood in terms of a melting point depression related to their thickness, as expressed in the Thomson–Gibbs equation[6], which in the case of laterally large lamellae reduces to

$$T_{m,l} = \Theta\left(1 - \frac{2\sigma_E}{\Delta H_f \rho_c l}\right) \tag{1}$$

Equation (1) relates the melting point, $T_{m,l}$, of a hard block lamellae of thickness l, to the thermodynamic melting point Θ of the infinite perfect crystal, the surface energy of the crystal σ_E, the heat of fusion ΔH_f and the crystal density ρ_c. Analysis of the mobile fraction with temperature allowed the hard segment domain size distribution to be determined. However, small angle X-ray scattering (SAXS) was required to fix the absolute distance scale. Note that since this model only involves the melting point depression arising from the size of the pure paracrystalline hard segment domains no assumptions need to be made about the larger scale morphology; that is the way in which these hard domains are embedded in the soft segment phase.

Melting will also cause profound changes in the n.m.r. properties of the ^{1}H spins, for example in the ^{1}H free induction decay (FID) through components with differing decay time constants. This, in principle, allows a similar analysis without the need for isotopic enrichment. Moreover, ^{1}H spin diffusion can then be used to estimate the mean domain size and provide a self consistent picture of the domain structure by n.m.r. measurements. One complication to this picture is that the resolution in the ^{1}H n.m.r. spectra does not allow the ready identification nor partitioning of magnetization seen in the FID as MDI, chain extender or polyether. Broadly speaking we can identify the fast decaying, gaussian like component seen in the ^{1}H FID, which corresponds to rigid ^{1}H spins, as coming from the paracrystals of hard segments while the slow decaying

* To whom correspondence should be addressed

exponential from a mobile ^1H spin represents the soft domains already above their T_g and hard domains which have melted.

Uncertainties naturally arise over the validity of this assumption and the resulting consequences on any analysis of the temperature variation in terms of a domain size distribution. In particular when the mobility of the soft segments approaches that of the hard segments this simple analysis of the ^1H FID will not be possible. Thus sensible results can only be expected when the smallest paracrystals associated with the hard segments melt at a temperature well above the T_g of the soft segments. A qualitative judgement can be made about the nature of the ^1H magnetization and thus any possible contribution of the soft segments to the rigid ^1H signal, by making use of selective ^{13}C n.m.r. experiments[7–9] where the phase is selected on the basis of its ^1H n.m.r. spin properties and this is then transferred into the ^{13}C spin system where identification can be made on the basis of the ^{13}C chemical shift.

In this paper a Thomson–Gibbs analysis is applied to the temperature variation of the ^1H FID of a polyurethane elastomer assuming a half and full gaussian distribution for the lamellar thickness of the hard blocks. The absolute distance scale is fixed by a ^1H spin diffusion measurement based on the Goldmann–Shen pulse sequence[10] and the validity of the partitioning of the FID is tested by selective ^{13}C n.m.r. experiments.

EXPERIMENTAL

Materials

The same polyurethane elastomer as used in the earlier ^2H n.m.r. and SAXS experiments was studied to permit an accurate comparison with these results. Previous ^2H n.m.r. experiments have shown that the melting of the hard domains caused by the heating cycle is reversible. In this elastomer the soft block phase is a bifunctional poly(ethylene-tetramethyleneadipate) with an average molecular weight of 2000 Da. The backbone of this commercial polyester from ICI plc (Daltocast TA20) consists of adipic acid/ethylene glycol/butanediol in a molar ratio equal to 2/1/1. The procedure for the synthesis of the deuterated elastomer is as follows: TA20 and 1,4-butanediol (1,4-BD) are dried under vacuum for several hours at 50°C. Just before use MDI-d_2 is distilled under vacuum and kept in an oven at 45°C. A polyol blend is made from TA20 (10.0 nmol–20.0 g) and 1,4-BD (25.0 mmol–2.25 g) both at 80°C by mixing them at 3000 rpm for 10 s. Next the MDI-d_2 (35.0 mmol–8.82 g) at 45°C is added to the polyol blend and everything mixed at 3000 rpm for 20 s and degassed under vacuum for 6 min to release the air bubbles. The reaction mixture is then poured into a shallow aluminium mould which has been treated with a mould release agent. The mould is put in an oven at 80°C for 16 h. Given the specific stoichiometry for the reactants, the average structure of the elastomer can be represented as shown in *Scheme 1*.

The mass fraction of the hard segments, calculated from the above composition, is 0.36. Assuming this mass fraction we can estimate that the fraction of the ^1H signal from the hard segments in the total ^1H signal intensity will be 0.28.

Solid state ^1H n.m.r.

The ^1H n.m.r. spectra were acquired on a Bruker MSL200 NMR spectrometer operating at 200.13 MHz. A solid echo pulse[11] sequence $[(\pi/2)_y - t_1 - (\pi/2)_x - t_2]$, combined with phase cycling and an echo delay of 8 μs, was used together with a pulse width of 3.0 μs. The r.f. amplitudes and phase orthogonality were checked prior to data acquisition using a standard multiple pulse tune up procedure on a H_2O sample. 4000 data points were acquired with a dwell time of 0.2 μs to ensure a faithful reproduction of the fast decaying component. Typically the sample was left to equilibrate for 1 h at the chosen temperature before collecting 1000 transients. A value of t_2 was chosen to ensure that data acquisition began on the top of the solid echo. Experimental errors for use in the FID analysis were estimated from the last 20 data points of the ^1H FID. The rigid fraction present at the chosen temperatures was found by fitting the ^1H FID to a gaussian and exponential decay using a non-linear least squares fitting program based on the Levenberg–Marquardt algorithm[12]. Calculations were carried out on a Tandon 286 PC with a Microsoft FORTRAN compiler. Chemical shift oscillations made analysis of the full ^1H FID unduly complex hence only the first 200 data points were used in the fitting procedure. Based on the time constraints determined in the fitting procedure this is equivalent to twice the effective decay time of the rigid hard block component. Since our sole concern was to determine the mobile fraction as a function of temperature from the decrease in the rigid fraction and not to determine the nature of the exponential decay this procedure is valid. Spin diffusion experiments were performed using a modified Goldman–Shen pulse sequence where the final $\pi/2$ pulse was replaced by a solid echo. A delay of 100 μs was used to ensure that complete dephasing of the short T_2 occurs, giving an initial magnetization gradient corresponding to magnetization only in the mobile or soft block component while the build up in the hard segment magnetization was followed out to a spin diffusion time of 100 ms. The actual recovery in the hard segment signal as a function of the spin diffusion time was determined by fitting the ^1H FID to a gaussian and exponential function, as in the variable temperature studies, and identifying the fast decaying gaussian function with the signal from the hard domains. Domain sizes were obtained by modelling the Goldman–Shen recovery curve on the basis of a simple two-region, one-dimensional morphology assuming a spin diffusion coefficient of $1 \times 10^{-16}\ m^2\ s^{-1}$ for the mobile domain and $4 \times 10^{-16}\ m^2\ s^{-1}$ for the hard domain[13].

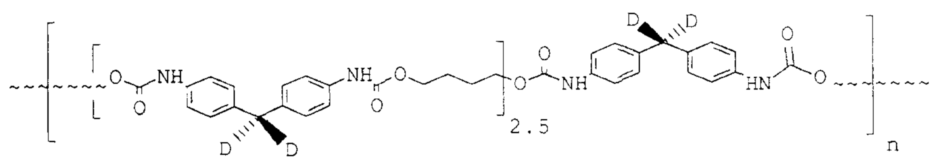

Scheme 1

RESULTS AND DISCUSSION

^{1}H n.m.r. FIDs were collected in the temperature range 294–390 K. At each temperature two components can be identified as expected. One, a slow decaying exponential characteristic of rapid quasi-isotropic motion increases with temperature and the other a fast decaying gaussian associated with ^{1}H spins in a rigid lattice decreases with temperature. The observed change in the relative fraction of the rigid and mobile components is consistent with the model of hard paracrystalline domains melting and dissolving into the soft phase. All fits to the experimental FIDs based on a gaussian and exponential function gave an error of less than 0.6%. Note that this does not correspond to a statistically acceptable χ^2, which would require a fitting error of less than 0.06%. In part this reflects a failure to recognize that the polymer dynamics are not single valued but determined by a distribution of correlation times thereby giving a distribution in time constants for the decays. At 294 K the FID fraction associated with the gaussian component was 0.23 in good agreement with that expected on the basis of the hard segment mass fraction, assuming it is completely rigid at this temperature. Furthermore because the soft segments are observed to have a T_g of 253.5 K by differential scanning calorimetry (d.s.c.) they should not contribute to the rigid ^{1}H signal. Accurate time constants for the exponential component were not obtained because of the restriction in the FID analysis to the first 200 data points. On the other hand the time constant for the gaussian component was found in the fitting procedure. Over the entire temperature range it shows very little variation; at 294 K it is 12.4 μs while at 389 K it is 14.7 μs. Both values are consistent with nearly the full second moment for the aromatic ring system, though some reduction must be taking place at higher temperature, indicating that the hard paracrystalline domains where they continue to exist remain largely unaffected by the increase in temperature. Evidence supporting the idea of a broad melting phenomenon is provided by differential scanning calorimetry where a broad endothermic transition is seen smeared out over a wide temperature range.

A quantitative description of the variation in melting points of crystallites in semi-crystalline polymers as a function of the lamellar thicknesses, is given by the Thomson–Gibbs equation[6], equation (1). In terms of equation (1), at any given temperature, the fraction of hard block lamellae that has melted will simply be the fraction of hard blocks with a lamellar thickness less than a defined value ($l < l_T$). Thus at low temperatures the mobile hard segment fraction corresponds to segments originally located in very thin lamellae and as the temperature is increased, thicker lamellae melt until finally all have melted. Modelling of the temperature variation in the mobile fraction requires an assumption be made about the nature of the domain size distribution. In the first instance a half gaussian was chosen as the distribution model for the hard block thicknesses. Using this distribution the probability of a given lamellar thickness l is given by

$$P(l) - \frac{1}{\sigma_l^* \sqrt{2\pi}} \exp\left[-\left(\frac{l-\mu^*}{\sigma_l^*\sqrt{2}}\right)^2\right] \qquad (3)$$

where * is used to signify that these parameters do not have their conventional meaning as the mean and standard deviation of the distribution. The true standard deviation of the half gaussian distribution is given by $0.603\sigma_l^*$. Rewriting the Thomson–Gibbs equation as

$$l = \frac{\alpha}{1 - T/\Theta} \quad \text{with} \quad \alpha = \frac{2\sigma_E}{H_f \rho_c} \qquad (4a, b)$$

Allows the gaussian variate to be expressed in terms of the three absolute temperatures, T, Θ, T_u, and thus gives the probability in terms of the hard domain melting point

$$\frac{l - \mu^*}{\sigma_l^* \sqrt{2\pi}} = \frac{\frac{1}{1-T/\Theta} - \frac{1}{1-T_{\mu^*}/\Theta}}{\xi\sqrt{2}} \quad \text{with} \quad \xi = \frac{\sigma_l^*}{\alpha} \qquad (5)$$

Experimentally the fraction of hard domains mobile at a given temperature T is measured. This corresponds to the fraction of hard block lamellae having a lamellar thickness less than that implying a melting point of T. To find this the half gaussian distribution is integrated from $T_{\mu*}$ to T, which is equal to

$$F(l < l_T) = 1 - \frac{\text{erfc}}{2}\left[\frac{\frac{1}{1-T/\Theta} - \frac{1}{1-T_{\mu^*}/\Theta}}{\xi\sqrt{2}}\right] \qquad (6)$$

With μ^* representing the lower end limit of the lamellar thicknesses, T_{μ^*} can be replaced by the highest temperature at which no mobile fraction is detected, which should be around 294 K. Θ is the thermodynamic melting point of an infinite crystal. Fitting of the observed mobile fraction to the calculated mobile fraction was based on a SIMPLEX routine[12] where each of the three variables T_{μ^*}, Θ and ξ in equation (4) are optimized. *Figure 1* shows the best fit to the experimental results using a half gaussian thickness distribution for the hard block lamellae: the corresponding values for the fitting parameters are $T_{\mu^*} = 249.6$ K, $\Theta = 454.4$ K and $\xi = 5.2$ with χ^2 of 53.4. Overall the fit poorly reproduces the low temperature data, in particular, the calculated minimum temperature T_{μ^*} is shifted significantly downwards from 294 K to 249.6 K. However, in contrast the thermodynamic melting point of Θ of 454.4 K agrees quite well with the melting point of the model compound of the hard segments[4], namely 465 K. The width of the distribution is determined by $\xi = 5.2$.

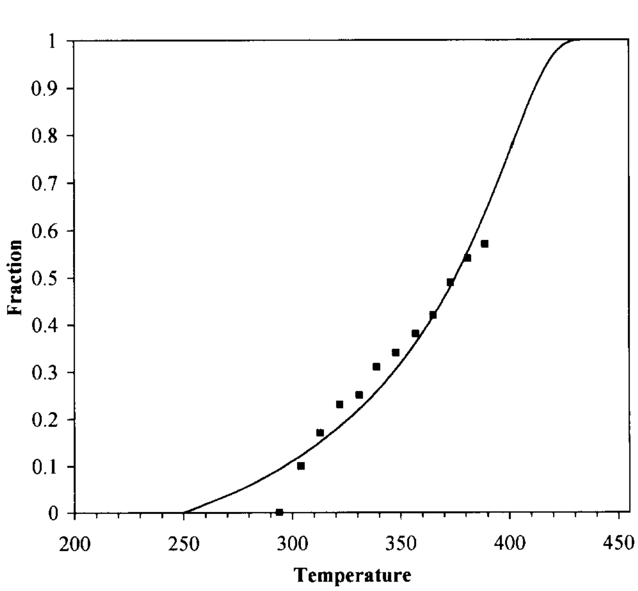

Figure 1 Fit of the mobile fraction, $F(l < l_T)$, against temperature using the Thomson–Gibbs equation and a half gaussian distribution for the hard block lamellae thicknesses

Given that the hard segments are formed in a polycondensation process, it is reasonable to propose that the thickness distribution should be more like a full gaussian than a truncated one. In this case the lamellar thickness distribution is given by a full gaussian distribution rather than a half one where σ_l and μ are the standard deviation and mean of the distribution respectively. In order to assure that the distribution contains only positive lamellar thicknesses the boundary condition $\mu - 3\sigma_l = l_{min}$ is introduced, with l_{min} the minimum lamellar thickness. The same reasoning as in the case of the half gaussian distribution can be applied for expressing the gaussian variate in terms of the absolute temperatures T_μ, Θ and T. However in this case T_μ is now the temperature at which 50% of the mobile fraction is present. According to this model, the fraction of molten hard block lamellae at temperature T is equal to

$$F(l < l_T) = 1 - \mathrm{erfc}\left[\frac{\frac{1}{1-T/\Theta} - \frac{1}{1-T_\mu/\Theta}}{\xi\sqrt{2}}\right] \quad (7)$$

Figure 2 shows a fit of the experimental results using a gaussian thickness distribution for the hard block lamellae. The best fitting parameters are $T_\mu = 376$ K, $\Theta = 493.9$ K and value of 1.54 for ξ. This model gives a χ^2 of 77.8 which is not so good as the half gaussian model. Particular faults with this model are that the thermodynamic melting temperature is significantly displaced from its expected value, while the low temperature behaviour is not properly represented. Despite having an estimate for ξ from both gaussian models it is impossible to calculate the absolute thickness distribution of the hard block lamellae from the temperature dependent solid state n.m.r. data alone because the value of α in equation (4b) is unknown.

The normalized Goldman–Shen recovery curve is shown in *Figure 3* and the domain sizes obtained from the modelling are 12.1 nm for the soft domain and 1.9 nm for the hard domains. One notable feature of the spin-diffusion experiments was that the limiting hard domain composition at 12.6% fell well below the 23.3% seen in the equilibrium solid-echo ^{1}H n.m.r. spectrum. This discrepancy calls into question the validity of using the spin diffusion experiment to establish the mean hard domain thickness. A comparison of the recovery in the hard domain magnetization observed experimentally with that computed on the basis of the domain sizes found by SAXS[4] and the equilibrium compositions show that at all times the recovery in the experimental ^{1}H n.m.r. magnetization is only *ca.* 58% of that expected for the true hard domain composition. This would appear to rule out any differential spin-lattice relaxation effects in the two domains. One possible explanation for the low limiting hard domain composition in the spin diffusion experiment is that substantial volumes of the soft block are in large domains (dimensions in excess of 100 nm) and not in such intimate contact with the hard domains as other soft segments involved in the hard/soft domain morphology. In other words the hard/soft domains are embedded within a soft segment matrix. Overall the magnetization recovery would then be a two stage process with the rapid initial increase in the hard domain signal followed by a much slower build up to the true equilibrium. Experimentally only the initial recovery is seen with spin-lattice relaxation effects preventing any observation of the slower recovery from the larger domains.

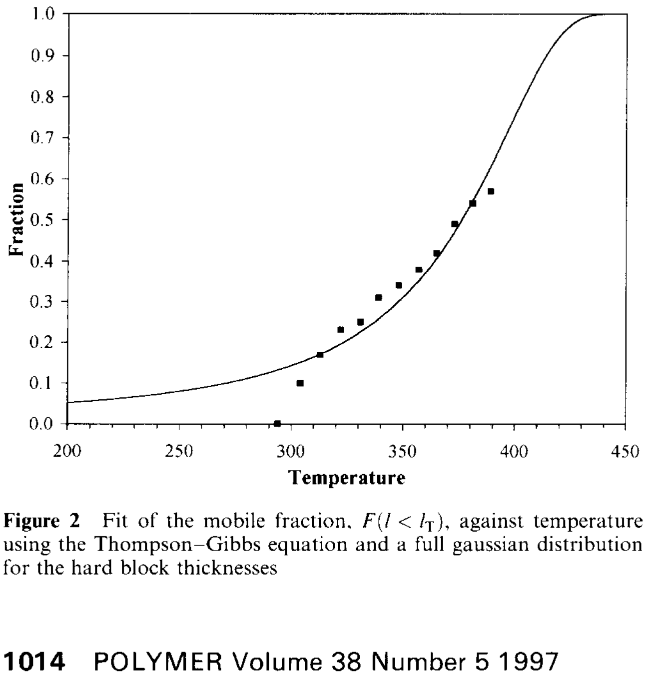

Figure 2 Fit of the mobile fraction, $F(l < l_T)$, against temperature using the Thompson–Gibbs equation and a full gaussian distribution for the hard block thicknesses

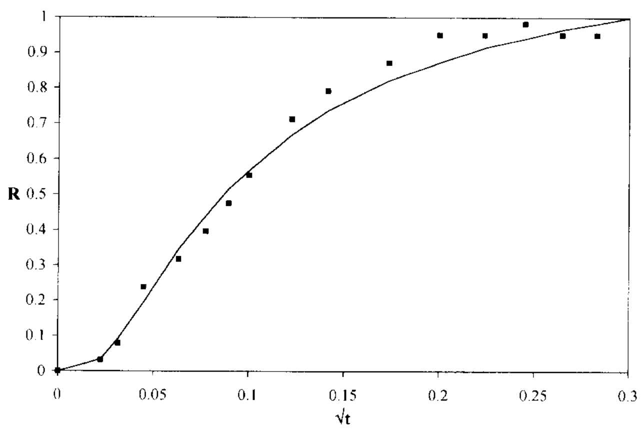

Figure 3 Magnetization recovery curve for the rigid component in the polyurethane elastomer. The solid line is the best fitted curve from the SIMPLEX routine with a soft block domain size of 12.1 nm and a hard block domain size of 1.9 nm. The recovered signal $R(t)$ is defined by $R(t) = [G(t) - G(0)]/[G(t = \infty) - G(0)]$, where $G(t)$ is the fraction of the Gaussian component after a spin diffusion time t

A close examination of the Goldman–Shen recovery curve reveals an induction period where little change takes place at first in the hard domain signal. The origin of this effect lies in the long preparation period used in this particular Goldman–Shen experiment. During this preparation period the hard domains act as relaxation sinks for the soft phase magnetization, depleting the magnetization on the soft side of the hard/soft interface. Consequently during the subsequent spin diffusion magnetization must initially be transported from the interior of the soft domain to the interface before it can appear in the hard domain.

In the light of the above difficulties with the ^{1}H spin diffusion experiments the average hard block lamella thickness of 3.0 nm must be taken from the SAXS results. Taking first the full gaussian model with the previously determined values for $T_\mu = 376$ K, $\Theta = 493.9$ K and $\xi = 1.54$ an estimate for the thus far unknown parameter α can be calculated as

$$\alpha_1 = l_h\left[1 - \frac{T_\mu}{\Theta}\right] = 3.00\left[1 - \frac{376}{494}\right] = 0.92 \quad (8)$$

From this value for α and the value of ξ (= 1.54) the standard deviation σ_l for the hard blocks can be obtained as $\sigma_l \approx 1.42$ nm. From the characteristic that a full width of a Gaussian distribution is approximately six standard deviations, the minimum and maximum value of the thickness distribution of the hard block lamellae is calculated to be

$$l_{\text{max}} \approx [l_h + 3\langle\sigma_l\rangle] = 8.0\,\text{nm}$$
$$l_{\text{min}} \approx [l_h - 3\langle\sigma_l\rangle] = 0\,\text{nm} \tag{9}$$

In view of the poor behaviour of the gaussian model at low temperatures it is not surprising that the minimum thickness is much smaller than the smallest possible hard segment length calculated from the XRD data[14], i.e. 1.2 nm, for a diphenylmethane structure terminated at both ends with a urethane (–NHCOO–) group. Similar calculations for the half gaussian distribution are somewhat more complicated because the relationship between the parameters determining the functional form for the probability density function and the statistical variables, namely the mean and standard deviation, of the distribution[15] have to be taken into account. Once this is done the average value for σ_l is found to be 1.48 nm, not too different from the full gaussian model. Despite the somewhat larger value for the standard deviation, the truncation condition in the half Gaussian distribution ensures an acceptable minimum thickness, namely 1.05 nm. The maximum thickness is 7.48 nm.

Judged on the basis of the χ^2 for the two models, the half gaussian is a better description of the hard segment size distribution. Although differences are seen between the models the actual hard domain thickness distributions derived are in good agreement and thus we can be confident that the hard block thickness distribution in this elastomer is quite narrow. A comparison of the parameters derived in the current ^{1}H n.m.r. study and those from the earlier ^{2}H work are shown in *Tables 1* and *2*.

The difference in the polymer dynamics shown by the ^{1}H and ^{2}H results at low temperature indicates that a rigid component, not associated with the MDI, melts at these temperatures. This rigid component may well represent an interphase region between hard and soft domains. In other respects the two sets of distribution parameters are in good agreement demonstrating that ^{1}H n.m.r. measurements can give domain size distributions despite the concerns over the correct partitioning of the ^{1}H FID into hard segment and soft segment magnetization.

Selective ^{13}C n.m.r. experiments were carried out with the aim of establishing the chemical identity of the two components seen in the ^{1}H FID. A reference ^{13}C cross-polarization magic angle spinning[16] (CP/MAS) n.m.r. spectrum of the polyurethane elastomer is shown in *Figure 4a*. Aromatic hard block resonances are clearly present while the intensity of the poly-ether soft segments are significantly attenuated from the intensity one might have expected on the basis of the relative mass fractions owing to the greater mobility of the soft segments. Although the greater mobility of the soft segments does make cross-polarization less effective by partially averaging the dipolar interactions it is instructive that we can still transfer magnetization from the ^{1}H spins to the ^{13}C spins in the mobile phase in such an experiment. Hence an additional selection stage is required to separate out the mobile and rigid components of the ^{1}H FID. From the preceding discussion it is also evident that the standard ^{13}C CP/MAS n.m.r. spectrum can only give a qualitative description of the elastomer. Clearer selection of the mobile phase can be made by adding a delay before spin-locking the ^{1}H magnetization. During this delay the ^{1}H signal will decay by T_2 relaxation and by choosing an appropriate delay all the ^{1}H magnetization associated with the short T_2 relaxation and by choosing an appropriate delay all the ^{1}H magnetization associated with the short T_2 component can be removed. Based on the time constant of 14 μs found for the gaussian decay in

Table 1 Comparison of the hard block distribution parameters

	Half-Gaussian		Gaussian	
	^{2}H	^{1}H	^{2}H	^{1}H
T_μ	294	249	375	376
Θ	465	454.4	493	493.9
ξ	3.35	5.2	1.18	1.55

Table 2 Comparison of the hard block domain sizes for a given probability distribution model assuming that the temperature dependence of the ^{2}H n.m.r. and ^{1}H n.m.r. is consistent with a range of hard block melting temperatures. Normalized sizes based on an average hard block thickness of 3.00 nm for ^{2}H and ^{1}H

	Half-Gaussian		Gaussian	
	^{2}H	^{1}H	^{2}H	^{1}H
α	0.545	0.472	0.72	0.92
l_{min} (nm)	1.53	1.05	0.5	0
l_{max} (nm)	6.33	7.44	5.6	8.1

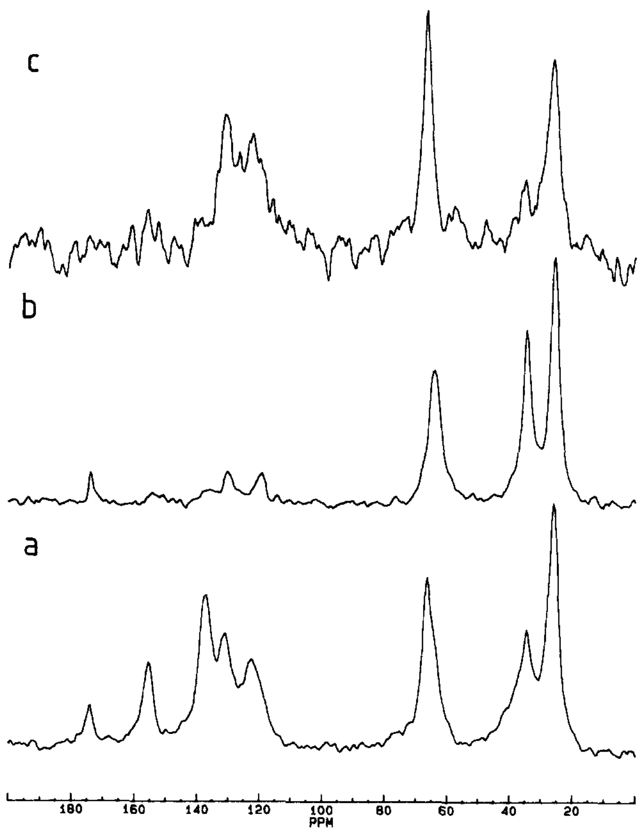

Figure 4 50.32 MHz ^{13}C CP/MAS n.m.r. spectra of a poly(ester-urethane) elastomer. Spinning speed of about 5 kHz. (a) Normal CP with a contact time of 2 ms, 1600 transients with a recycle delay of 3 s. (b) Delayed spin-lock CP with a delay time of 100 μs and a contact time of 2 ms, 6000 transients with a recycle delay of 3 s. (c) Short contact time, 20 μs, CP, 1200 transients with a recycle delay of 3 s

the ^{1}H FID a T_2 relaxation delay of 100 μs was used. With this delay the contribution from the rigid component will be negligible. In this selective ^{13}C n.m.r. spectrum, *Figure 4b*, most of the intensity in the aromatic region is lost, confirming the assignment of this signal at room temperature to the polyether. Significantly, though, not all of the aromatic intensity is lost demonstrating that even at 300 K some of the hard block lies in a mobile phase; confirming the observation of a mobile hard segment fraction by ^{2}H n.m.r. at this temperature. In addition resonance overlap between the chain extender and the soft segment means that it is not possible to say what contribution the chain extender makes to the mobile ^{1}H signal. A clean identification of the short component is hindered by the cross polarization of the mobile phase. Despite the fact we can greatly reduce the interference by reducing the contact time in the cross-polarization pulse sequence we cannot so confidently eliminate it totally. (The time constant describing the rate at which the signal builds up, T_{CH}, depends on the magnitude of the dipolar coupling[17]). However, this will also bias the ^{13}C n.m.r. spectrum against quaternary carbons even in a rigid phase since these too have long T_{CH}. A short contact time ^{13}C CP/MAS n.m.r. spectrum, $\tau = 20\,\mu$s, is shown in *Figure 4c*, here we can see both the aromatic MDI and chain extender with very little evidence for soft segments. We can therefore be confident that the rigid ^{1}H signal does arise principally from the hard segments and chain extender.

CONCLUSIONS

The ^{1}H n.m.r. FID were described in terms of a rigid and highly mobile component. A model was proposed in which the melting of the hard block lamellae is related to their thickness using a Thomson–Gibbs equation. Of the two distribution functions used to describe the hard block thicknesses, the half gaussian one gave the best correlation between the ^{2}H n.m.r. data, the SAXS data, the experimentally determined thermodynamic melting point of the hard blocks, the XRD data and the estimated thickness distribution for the soft block lamellae. Little evidence was seen for a rapid quasi-isotropic motion in the hard blocks which would be necessary if the temperature dependence of the hard segment mobility is interpreted as an increase of dynamic freedom within the solid hard block domains. Spin diffusion experiments based on the Goldman–Shen pulse sequence were unsuccessful at providing a mean hard domain size because only 58% of the expected hard domain signal was seen. While this can be attributed to a heterogeneous morphology where a substantial fraction of the soft block does not contribute to the hard/soft domain structure further work on other samples is necessary to assess the general validity of this conclusion. Selective ^{13}C n.m.r. experiments confirm that the slow decaying component of the ^{1}H FID is associated with the soft segments as well as demonstrating that a small fraction of the hard segments are highly mobile even at 300 K. This fraction corresponds to the hard segments lying in the smallest domains. On the other hand the fast decaying component of the ^{1}H FID is associated with the hard segments; MDI and butanediol chain extender.

ACKNOWLEDGEMENT

We thank ICI Polyurethanes for permission to publish this work

REFERENCES

1 Saunders, J. H. and Frisch, K. C. 'Polyurethanes: Chemistry and Technology', Wiley Interscience, New York, 1962
2 McBrierty, V. J. *Faraday Discuss. Chem. Soc.* 1979, **68,** 78
3 Assink, R. A. *Macromolecules* 1978, **11,** 1233
4 Clayden, N. J., Nijs, C. L. and Eeckhaut, G. J. *Macromolecules* (submitted)
5 Koberstein, J. T. and Russell, T. P. *Macromolecules* 1986, **19,** 714
6 Wunderlich, B. *Chem. Phys.* 1958, **29,** 1395
7 Clayden, N. J. *Polymer* 1992, **33,** 3145
8 Bunn, A., Clayden, N. J. and Kemmish, D. J. *Macromolecules* 1993, **26,** 6138
9 Clayden, N. J. and Smyth, G. *Magn. Reson. Chem.* 1995, **33,** 710
10 Goldman, M. and Shen, L. *Phys. Rev.* 1966, **144,** 321
11 Powles, J. G. and Mansfield, P. *Phys. Lett.* 1962, **2,** 58
12 Press, W. H., Flannery, B. P., Teukolsky, S. A. and Vettering, W. T. 'Numerical Recipes, The Art of Scientific Computing', Cambridge University Press, New York, 1988
13 Cheung, T. T. P. *Phys. Rev.* 1981, **B23,** 1404
14 Quay, J. R., Blackwell, J., Lee, C. D., Hespe, H. and Born, L. J. *Macromol. Sci.-Phys.* 1985, **B24,** 61
15 Johnson, N. L. and Kotz, S. 'Distributions in Statistics, Continuous Univariate Distributions—1', Houghton Mifflin, Boston, 1970
16 Komoroski, R. A. (Ed.) 'High Resolution NMR Spectroscopy of Synthetic Polymers in Bulk', VCH, Orlando, FL, 1989
17 Mehring, M. 'Principles of High Resolution NMR in Solids', Springer-Verlag, Berlin, 1982